

Available online at [www.sciencedirect.com](http://www.sciencedirect.com)

journal homepage: [www.elsevier.com/locate/ajps](http://www.elsevier.com/locate/ajps)

## Original Research Paper

# Topical delivery of acetazolamide by encapsulating in mucoadhesive nanoparticles



Satish Manchanda<sup>\*</sup>, Pravat Kumar Sahoo

Delhi Institute of Pharmaceutical Sciences and Research (DIPSAR), Pushp Vihar Sector III, MB Road, New Delhi 110017, India

### ARTICLE INFO

#### Article history:

Received 29 December 2016

Accepted 27 April 2017

Available online 16 May 2017

#### Keywords:

Acetazolamide

Chitosan

STPP

Ocular hypertension

Mucoadhesion

### ABSTRACT

The intent of this study was to provide topical delivery of acetazolamide by preparing chitosan-STPP (sodium tripolyphosphate) nanoparticles of acetazolamide and evaluate the particle size, zeta potential, drug entrapment, particle morphology; *in vitro* drug release and *in vivo* efficacy. The particles showed sustained *in vitro* drug release which followed the Higuchi kinetic model. The results indicate that the nanoparticles released the drug by a combination of dissolution and diffusion. The optimised formulation was having particle size  $188.46 \pm 8.53$  nm and zeta potential  $+36.86 \pm 0.70$  mV. The particles were spherical with a polydispersity index of  $0.22 \pm 0.00$ . Powder X-ray diffraction and differential scanning calorimetry indicated diminished crystallinity of drug in the nanoparticle formulation. In the *in vitro* permeation study, the nanoparticle formulation showed elevated permeation as compared to that of drug solution with negative signs of corneal damage. *In vitro* mucoadhesion studies showed  $90.34 \pm 1.12\%$  mucoadhesion. The *in vivo* studies involving ocular hypotensive activity in rabbits revealed significantly higher hypotensive activity ( $P < 0.05$ ) as compared with plain drug solution with no signs of ocular irritation. The stability studies revealed that formulation was quite stable.

© 2017 Shenyang Pharmaceutical University. Production and hosting by Elsevier B.V. This is an open access article under the CC BY-NC-ND license (<http://creativecommons.org/licenses/by-nc-nd/4.0/>).

## 1. Introduction

The development of operative drug delivery systems that can convey and deliver a drug specifically and securely to its site of action is becoming a highly imperative investigation area for pharmaceutical researchers. Consequently, promising

ways of delivering poorly soluble drugs, peptides and proteins etc. have been concocted. Ocular drug delivery is one of the most fascinating and puzzling endeavours faced by the pharmaceutical scientist, because of the precarious and pharmacokinetically explicit environment that exists in the eye. The anatomy, physiology and biochemistry of the eye render this organ exquisitely impervious to foreign substances [1]. In

<sup>\*</sup> Corresponding author. Delhi Institute of Pharmaceutical Sciences and Research (DIPSAR), Pushp Vihar Sector III, MB Road, New Delhi 110017, India. Tel.: +91 9810808745; Fax: +91 11 29554503.

E-mail address: [manchandasatish@gmail.com](mailto:manchandasatish@gmail.com) (S. Manchanda).

Peer review under responsibility of Shenyang Pharmaceutical University.

<https://doi.org/10.1016/j.ajps.2017.04.005>

1818-0876/© 2017 Shenyang Pharmaceutical University. Production and hosting by Elsevier B.V. This is an open access article under the CC BY-NC-ND license (<http://creativecommons.org/licenses/by-nc-nd/4.0/>).

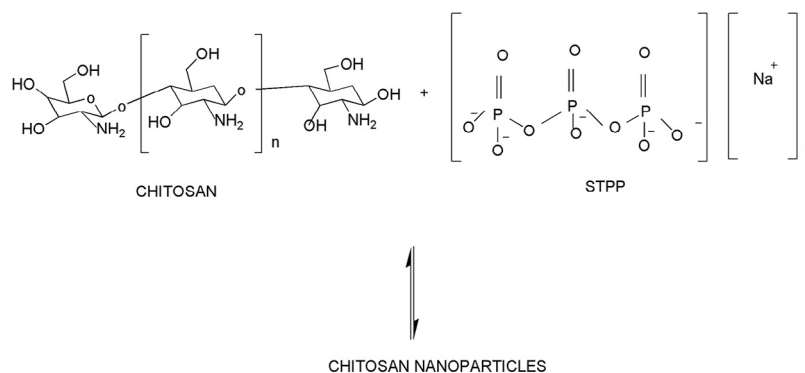


**Fig. 1 – Formulation of nanoparticles by ionic gelation.**

the formulation of novel topical ocular dosage forms, a great attention is now being devoted to new drug delivery systems that can ensure a localized effect, have convenience of a drop and at the same time increase the corneal permeability of poorly permeable drugs [2]. In order to conquer the problems of conventional ocular therapy, such as short residence time, loss of drug through nasolacrimal drainage, impermeability of corneal epithelium and recurrent instillation; newer topical delivery systems are being explored by many researchers [3].

Acetazolamide (ACZ), a carbonic anhydrase inhibitor and chemically a sulphonamide, is used orally for the diminution of intraocular pressure (IOP) in patients suffering from glaucoma. Large oral doses of ACZ are used to obtain the desired lowering in IOP which usually leads to systemic side effects, the most common of which are diuresis and metabolic acidosis [4]. Most of the patients are incapable to endure the side effects of acetazolamide and hence they withdraw the therapy. As a result, topical administration of ACZ is required over systemic administration. Thus, a number of scientists sought to develop an effective topical formulation which includes use of high drug concentration (2.5–10% w/v), use of viscolising agents (PVA, HPMC), use of penetration enhancers (EDTA), use of complexing agents (hydroxyl propyl- $\beta$ -cyclodextrin) [5], entrapment in particulate drug delivery carriers [3,6] but promising results were not obtained in terms of intensity of decrease of IOP and side effects. The restriction in development of topical formulation of acetazolamide are its low solubility, its inadequate corneal penetration ( $\log P = 0.3$ ).

Chitosan (CS) the second most copious biopolymer in natural world next to cellulose, derived from the exoskeleton of shrimps, other crustaceans, insects, fungi etc. and is one of the very few positively charged natural biopolymers existing in the biosphere [7,8]. CS is having structure connexion to cellulose and poised of linear  $\beta$ -(1 $\rightarrow$ 4)-linked monosaccharide. CS is manufactured by partial deacetylation of chitin from crustacean shells. The primary amine groups afford special property that make CS very expedient in pharmaceutical applications [9]. The cationic polysaccharide CS has some important possessions such as mucoadhesivity, biocompatibility, and non toxicity which render it an interesting biomaterial. From a physicochemical perspective, CS has the distinct feature of gelling upon contact with anions thus sanctioning the realisation of beads under very mild conditions

[10,11] and this process is termed as Ionic/Ionotropic gelation (Fig. 1). CS has been used for sustained release systems, preparation of mucoadhesive formulations, improvement of the dissolution rate of poorly soluble drugs, drug targeting and enhancement of peptide drug absorption [12]. Ionic gelation, complex coacervation, emulsion cross-linking and spray-drying are approaches usually used for the preparation of CS nanoparticles. Most researchers adapt the ionic gelation method developed by Calvo et al. using CS and TPP for the incorporation of proteins.

In the present study, mucoadhesive chitosan-sodium tripolyphosphate nanoformulations of acetazolamide, to be applied topically, were formulated and evaluated for their in vitro and in vivo performance. Stability studies were also carried out to investigate the leaching of drug from nanoformulations during storage [3,13].

## 2. Material and methods

### 2.1. Material

Acetazolamide (ACZ), chitosan high molecular weight (CS-HMW) and chitosan low molecular weight (CS-LMW) were purchased from Sigma Aldrich (USA). Sodium tripolyphosphate (STPP) was purchased from HiMedia (Mumbai, India) and mannitol was purchased from SD-Fine (Mumbai, India). All the solvents used were of HPLC grade. Acetic acid was procured from Central Drug House (Delhi, India) whereas Acetonitrile was obtained from Merck (India). The water used was distilled and deionised by using Millipore (ELIX) system.

### 2.2. Methods

#### 2.2.1. Preparation of chitosan (CS) and sodium tripolyphosphate (STPP) solutions

Chitosan (HMW and LMW) was dissolved in different concentrations (1 mg/ml, 2 mg/ml and 3 mg/ml) in 1% v/v acetic acid aqueous solution to harvest the solutions of CS of concluding concentration of 0.1% w/v, 0.2% w/v and 0.3% w/v. On the other hand an aqueous solution of STPP of concentration 0.1% w/v was finalised for preparing nanoformulations.

### 2.2.2. Formulation of acetazolamide (ACZ) loaded nanoparticles

Iontropic gelation method was used which was described previously with minor amendments. Concisely, under continuous magnetic stirring (1000 rpm) at room temperature, 4 ml of STPP solution was slowly added to 10 ml CS solution to acquire nanoparticles promptly by the mechanism of ionotropic interaction of chitosan with polyanions of STPP [14]. Magnetic stirring was sustained for 2h at room temperature for the system stabilisation. The nanoparticles so obtained were then lyophilised in lyophilizer (Allied Frost, New Delhi) after incorporation of 5% Mannitol as cryoprotectant and stored for further analysis. ACZ was dissolved in CS solution prior to STPP solution addition, for encapsulating the drug within the core of nanoparticles. The formulations of CS-LMW (0.1% w/v, 0.2% w/v and 0.3% w/v) and STPP (0.1% w/v) were coded as AS1, AS2 and AS3. On the other hand formulations of CS-HMW (0.1% w/v, 0.2% w/v and 0.3% w/v) and STPP (0.1% w/v) were coded as AS4, AS5 and AS6. In every formulation the concentration of drug was kept 0.1% w/v.

### 2.2.3. Characterization of nanoparticles

**2.2.3.1. Percent drug entrapment.** Ten milligrams of lyophilized nanoparticles were suspended in 10 ml of distilled water (DW) by sonication in ultra-bathsonicator (Metrex). This suspension is then centrifuged (Remi) at 12,000 rpm for 30 min and supernatant was analysed for the drug content by in house developed and validated HPLC method at 265 nm, having limit of detection (LOD) and limit of quantification (LOQ) of 37.60 ng/ml and 0.11 µg/ml respectively. For the analysis of ACZ by HPLC, C8H column (250 mm × 4.6 mm) was used as stationary phase and potassium dihydrogen phosphate buffer (pH 3), Acetonitrile and water in a ratio 30:20:50 as mobile phase with a flow rate of 0.8 ml/min, injection volume of 20 µl, run time of 10 min and optimized RT of 6.8 [15].

The entrapment efficiency was then calculated by the following equation:

% Entrapment Efficiency

$$= \frac{\text{Initial Amount of Drug} - \text{Drug in supernatant}}{\text{Initial Amount of Drug}} \times 100$$

**2.2.3.2. Particle size and zeta potential.** Lyophilised nanoparticles were disseminated in water and sonicated in ultrasonicator bath for 30 sec. Particle size, zeta potential and PDI (polydispersity) index was then analysed by Zetasizer Nano ZS-90 (Malvern Instruments, Worcestershire, UK) equipped with the DTS software. Each value quoted was the mean of determinations of three independent samples.

**2.2.3.3. Particle morphology (transmission electron microscopy).** Morphological evaluation of the freeze-dried nanoparticles was performed using transmission electron microscopy (TEM) (FEI, Netherlands). Samples were immobilized on copper grids. They were dried at  $25 \pm 2$  °C and then were examined using TEM without being stained.

**2.2.3.4. Powder X-ray diffraction (PXRD) studies.** PXRD patterns of samples were recorded with X-ray diffractometer

(Bruker D8, Discover) using Cu radiation (wavelength 1.54), in the diffraction angle range of 5–40° 2θ. The angle range was having 1751 steps and it took 0.9 s/step with an increment of 0.02.

**2.2.3.5. FTIR-ATR studies.** IR spectra of samples were recorded using a FTIR-ATR spectrophotometer (Bruker) in the range of 4000–400 cm<sup>-1</sup>.

**2.2.3.6. Differential scanning calorimetry (DSC).** DSC analysis was performed using a DSC TA-60 (Shimadzu, Tokyo, Japan) calorimeter. Samples were heated in sealed aluminium pans under nitrogen flow (50 ml/min) at a scanning rate of 10 °C/min from 40 °C to 300 °C. An empty aluminium pan was used as the reference pan.

**2.2.3.7. In-vitro drug release.** For in-vitro studies, 1 ml of freshly prepared nanosuspension/drug solution corresponding to 0.1% w/v of drug was sealed in the Dialysis membrane tube (HiMedia, India) with the help of dialysis closure clips (HiMedia, India) and made to sink in a beaker containing 100 ml of Sorenson Phosphate buffer pH 7.4 which served as dissolution media. The dissolution media was stirred continuously with help of Teflon coated magnetic bar at speed of 50 rpm. Thereafter samples of 5 ml volume were withdrawn at the specific time intervals (30, 60, 120, 180, 240, 360, 480 min) and replaced with the fresh dissolution media to maintain the sink conditions [16]. The samples withdrawn were then analysed by HPLC method at 265 nm.

**2.2.3.8. Ex-vivo transcorneal permeation.** Modified Franz diffusion cell was used for reviewing permeation across excised goat cornea. Intact eyeballs of goat were acquired from the local slaughter (Khanpur, Delhi) within 1 h of slaughtering of animal. The cornea was then cautiously detached from the eyeball, leaving extra 2–4 mm of epithelial membrane around the cornea, for the appropriate mounting over diffusion cell [17,18]. The cornea was then mounted over the Modified diffusion cell keeping epithelial membrane towards donor compartment. Receptor chamber was filled with 10 ml of Sorenson phosphate buffer (pH 7.4) on the other hand donor chamber contained 1 ml of nanosuspension/solution comparable to 0.1% w/v of drug. After 2h sample was withdrawn from the donor compartment and analysed for the drug content permeated by HPLC method at 265 nm and percent drug permeation was calculated by the equation:

% Corneal Permeation

$$= \frac{\text{Amount of Drug Permeated In Receptor Chamber}}{\text{Initial Amount Of Drug In Donor Compartment}} \times 100$$

Percent corneal hydration was also calculated after cutting the extra 2 mm epithelial tissue and keeping the cornea in an hot air oven at 90 °C overnight after moistening in 1 ml methanol. The percent corneal hydration was calculated by the following equation [19,20]:

% Corneal hydration

$$= \frac{\text{Weight of moist cornea} - \text{Weight of dried cornea}}{\text{Weight of moist cornea}} \times 100$$

2.2.3.9. *Ex-vivo mucoadhesion studies.* The pig mucin (Himedia, Mumbai, India) suspension was prepared in 0.05 M saline phosphate buffer (pH 7.4). Placebo CS-NPs and drug loaded CS-NPs were mixed with 1 ml of mucin suspension and incubated at 37 °C for 30 min and kept for 24 h at room temperature. The samples were centrifuged in cooling centrifuge (12,000 rpm, 30 min); supernatant was collected and quantified free pig mucin by UV spectrophotometer (Perkin Almer) at 251 nm [21,22]. The binding efficiency of mucin with CS-NPs was calculated by following equation:

$$\% \text{ Mucoadhesion} = \frac{\text{Total Mucin Concentration} - \text{Mucin Concentration In Supernatant}}{\text{Total Mucin Concentration}} \times 100$$

### 2.3. In-vivo studies

#### 2.3.1. Ocular hypotensive efficacy

The normotensive rabbits were used to compare the ocular hypotensive activity of acetazolamide-loaded NPs with the aqueous solution containing equivalent amount of acetazolamide (positive control). The experimental protocol was designed and approval of Institutional Animal Ethics Committee (IAEC) was obtained. A group of three animals weighing 2–2.5 kg was used for each study [23–26]. Animals were housed in institutional animal house under standard conditions with free access to food and water. Each rabbit of Group I served as the control and received 50 µl of Normal saline (0.9% w/v) vehicle while the Group II and Group III received 50 µl of acetazolamide (0.1% w/v) ophthalmic solution in normal saline or 50 µl of acetazolamide (0.1% w/v) nanosuspension in normal saline respectively. Schiötz tonometer was used to measure the IOP in conscious rabbits. A volume of 50 µl of solution of lignocaine HCl (2% w/v) was used as a local anaesthetic. The resting IOP level was measured in all the animals before drug administration. The dose of acetazolamide administered was 1 mg either in the nano-formulation or in the solution form. A single 50 µl drop was instilled into the experimental eye at time 0, and the IOP was measured at 0.5, 1, 2, 3, 4 and 5 h after drug administration [23,25]. The change in IOP ( $\Delta$ IOP) was determined by the following equation:

$$\Delta \text{IOP} = \text{IOP}_{\text{Dosed Eye}} - \text{IOP}_{\text{Control Eye}}$$

#### 2.3.2. Determination of ocular irritation index

The ocular irritancy test was conducted as per the Modified Draize Test on a group of 3 New Zealand albino rabbits. Fifty micro litres of nano formulation was instilled into the lower cul-de-sac of the eye of each rabbit with the help of needleless syringe. The untreated contra-lateral eye was used as a control. The eyelids were gently held together for about 10 s for avoiding the loss of instilled solution. Each animal was observed for ocular reactions (redness, discharge, conjunctival chemosis, iris and corneal lesions) at 5, 10, 15, 30 min and 1, 2, 3, 6, 9, 12, 24 h post instillation. The ocular irritancy test was performed by providing 0 (absence) to 4 (highest) grades on clinical evaluation scale. Overall ocular irritation index (Iirr) was calculated by summing up the total clinical evaluation scores over the

observation time points. A score of 2 or 3 in any category or Iirr more than 4 was considered as an indicator of clinically significant irritation. The observation regarding the ocular irritation was noted for normal saline and ACZ loaded optimized nanoformulation [6].

### 2.4. Stability studies on optimized formulation

Freeze dried NPs were stored in screw capped glass bottles wrapped with aluminium foil and subjected to accelerated stability testing by exposing the particles at 40 °C and 75% RH. The long term stability study was conducted by storage at room temperature. Samples kept under accelerated storage condition were withdrawn at 0, 1.5, 3 and 6 months and drug content was estimated. Similarly, samples stored at room temperature were withdrawn at 0, 3, 6 and 12 months and analyzed for drug content [3,6,13,27–29].

### 2.5. Statistical analysis

Statistical calculations were done by one-way analysis of variance (ANOVA) followed by Dunnett's test or Student's t-test using Graph Pad Prism 5 software (Graph Pad Software Inc., San Diego, CA). A P value < 0.05 was considered significant.

## 3. Results and discussion

### 3.1. Results

#### 3.1.1. Percent drug entrapment

In the present study, the % drug entrapment ( $\pm$ SD) for AS1, AS2, AS3 formulations were found 74.55  $\pm$  0.01, 69.31  $\pm$  0.03, 60.90  $\pm$  0.02 respectively and for AS4, AS5 and AS6 percent entrapment were 80.02  $\pm$  0.02, 76.01  $\pm$  0.03, 73.77  $\pm$  0.04 respectively.

#### 3.1.2. Particle size and zeta potential

The individual values for particle size (nm  $\pm$  SD) for different formulations i.e. AS1, AS2, AS3, AS4, AS5 and AS6 were found to be 161.90  $\pm$  3.25, 188.46  $\pm$  8.53, 220.56  $\pm$  4.49, 239.66  $\pm$  3.90, 264.2  $\pm$  9.73 and 289.40  $\pm$  6.36 respectively whereas the values for Zeta potential (mV  $\pm$  SD) were + 24.16  $\pm$  0.45, + 36.86  $\pm$  0.70, + 31.43  $\pm$  0.56, + 28.9  $\pm$  0.5, + 33.46  $\pm$  0.86, and + 32.43  $\pm$  0.47 respectively. The values of PDI for different formulations AS1, AS2, AS3, AS4, AS5 and AS6 were 0.23  $\pm$  0.00, 0.22  $\pm$  0.00, 0.29  $\pm$  0.00, 0.27  $\pm$  0.00, 0.31  $\pm$  0.00 and 0.32  $\pm$  0.00 respectively.

#### 3.1.3. Particle morphology

The shape of particles was analyzed by TEM, which revealed discrete spherical shape (Fig. 2). TEM images revealed the particles size of the optimized formulation (AS2) was < 200 nm. The result of TEM was in agreement with the particle size measured by dynamic light scattering.

#### 3.1.4. Powder X-ray diffraction (PXRD) studies

Fig. 3 displays the X-ray diffractograms of samples. Acetazolamide showed the characteristic peaks at 9.90°, 16.38°, 19.84°, 19.94°, 29.96° and 30.14° 2 $\theta$  while diffractogram of mannitol showed the characteristic peaks at 14.56°, 18.76°, 20.40°, 21.08°



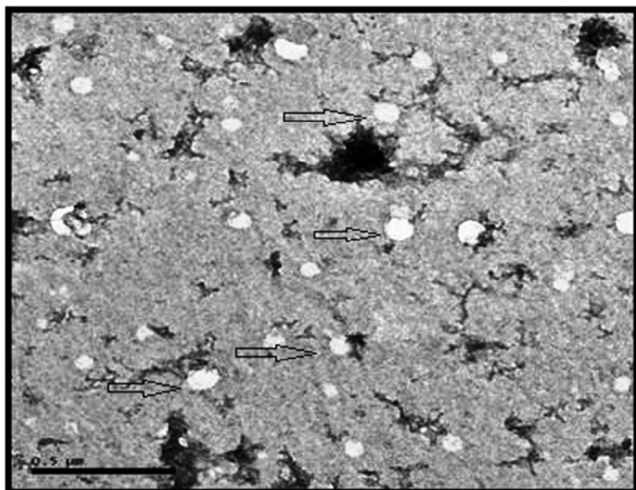


Fig. 2 – Transmission electron micrograph (TEM) image of optimised nanoformulation.

and  $29.46^\circ 2\theta$ . The diffractogram of STPP also exhibited significant peaks which were obtained at  $18.82^\circ$ ,  $19.40^\circ$ ,  $19.82^\circ$ ,  $24.78^\circ$ ,  $26.66^\circ$ ,  $33.33^\circ$ ,  $34.16^\circ$ ,  $34.56^\circ$  and  $37.14^\circ 2\theta$ . On the other hand no sharp peak was observed in the diffractograms of chitosan, while nanoformulation's diffractograms exhibited sharp peaks similar to that of mannitol.

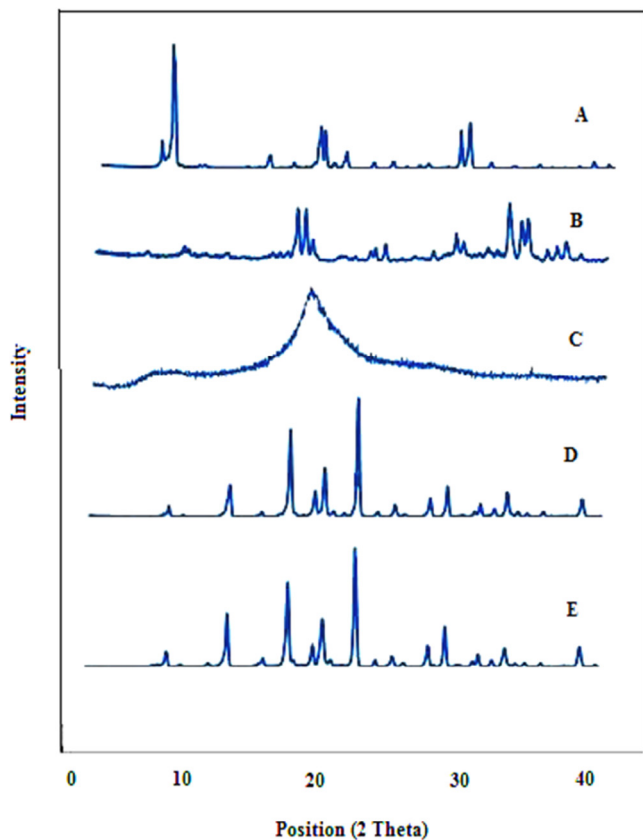


Fig. 3 – PXRD (A) drug (B) sodium tripolyphosphate (C) chitosan (D) mannitol (E) formulation.

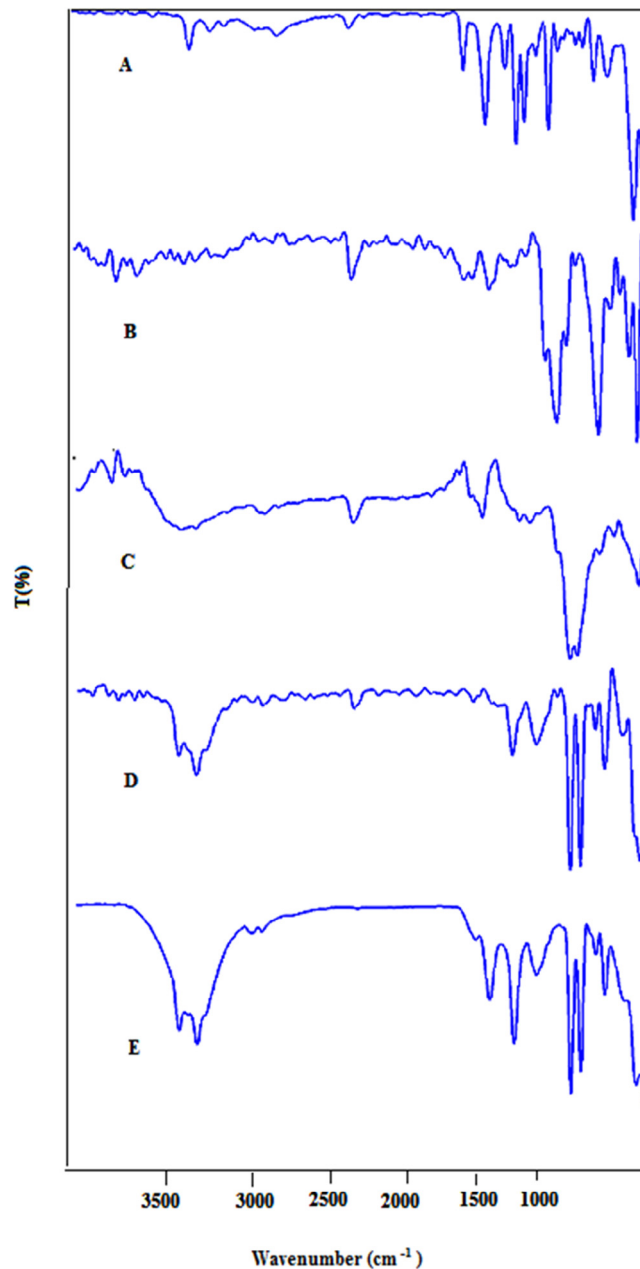
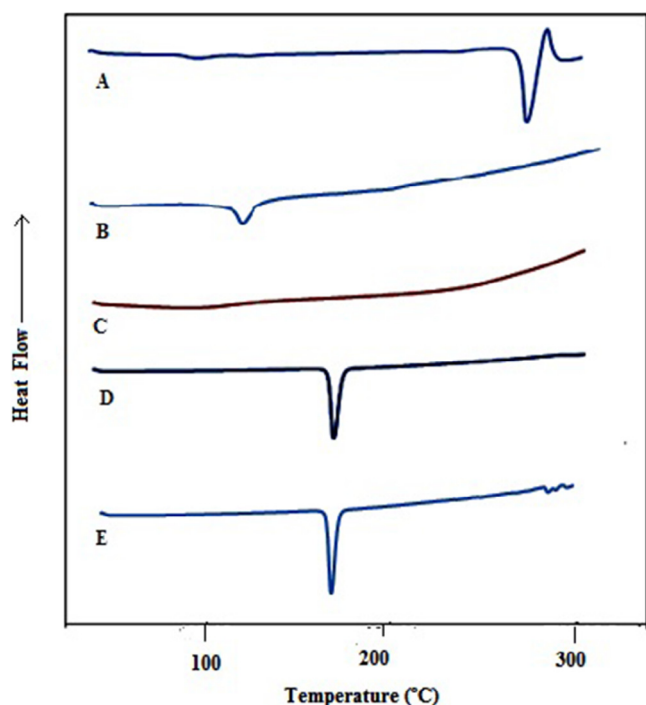


Fig. 4 – FTIR images of (A) drug (B) sodium tripolyphosphate (C) chitosan (D) mannitol (E) formulation.

### 3.1.5. FTIR-ATR studies

The FT-IR spectrum (Fig. 4) of ACZ gave signals at  $3296.88$  and  $3174.70$   $\text{cm}^{-1}$  from the N-H stretching of the secondary amine. The presence of absorption at  $1678.21$   $\text{cm}^{-1}$  was attributed to the C=O stretching of the carboxyl groups. The characteristic peak at  $1173.81$   $\text{cm}^{-1}$  were attributed to the S=O stretching of sulfonyl groups. S-N stretching absorption was observed at  $907.12$   $\text{cm}^{-1}$ . Characteristic chitosan peaks were observed at  $1645.68$   $\text{cm}^{-1}$  for the amide I band (C=O stretching),  $1565.97$   $\text{cm}^{-1}$  for the amide II band (N-H in plane deformation coupled with C-N stretching), and  $1075.08$   $\text{cm}^{-1}$  (C-O-C stretching). FTIR spectra of STPP has different characteristic peaks at  $1139.72$   $\text{cm}^{-1}$  (symmetric and antisymmetric stretching vibrations in PO<sub>2</sub> group) and  $895.29$   $\text{cm}^{-1}$  (stretching of the P-O-P bridge). Spectrum of



**Fig. 5 – DSC of (A) drug (B) sodium tripolyphosphate (C) chitosan (D) mannitol (E) formulation.**

mannitol showed OH stretching at  $3394.12\text{ cm}^{-1}$ , OH in plane bending at  $1419.19\text{ cm}^{-1}$ , C = O stretching at  $1078.92\text{ cm}^{-1}$  and OH out of plane bending for alcohol at  $701\text{ cm}^{-1}$ , whereas the spectrum of nanoformulations didn't show any characteristic peak of ACZ.

### 3.1.6. DSC

The DSC thermograms of samples are presented in Fig. 5. The thermogram of acetazolamide is characterized by a sharp melting endotherm at  $261\text{ }^{\circ}\text{C}$ . The thermal curve of chitosan is characterized by a broad endotherm without any sharp peak while thermogram of STPP showed a small endotherm at  $115.01\text{ }^{\circ}\text{C}$ . The thermal behaviour of mannitol is characterized by an endothermic peak at  $167.04\text{ }^{\circ}\text{C}$ . The thermogram of nanoformulations (AS2) exhibited a small endotherm at  $167\text{ }^{\circ}\text{C}$ .

### 3.1.7. In-vitro drug release

Fig. 6 compares the in vitro release of acetazolamide from the CS based nanosuspensions. The release of acetazolamide was assessed by dialysis, using Sorenson's phosphate buffer (pH 7.4) as the release medium. The NP formulations made with CS LMW (AS1, AS2, and AS3) showed  $44.08 \pm 2.38\%$ ,  $37.18 \pm 0.04\%$  and  $32.41 \pm 0.39\%$  drug release respectively in 8 h. On the other hand nanoformulations made with CS HMW (AS4, AS5, AS6) showed  $39.19 \pm 4.55\%$ ,  $34.27 \pm 0.36\%$  and  $30.80 \pm 1.61\%$  drug release respectively while  $98.72 \pm 6.25\%$  drug diffused into the release medium from an aqueous solution of the drug (0.1% w/v) used as a control. The release data of optimized formulation was fitted into various kinetic models like zero-order, first-order, Higuchi, Korsmeyer-Peppas and Hixson Crowell equations in order to determine the release mechanism and regression coefficients ( $R^2$ ) [30]. The release of acetazolamide

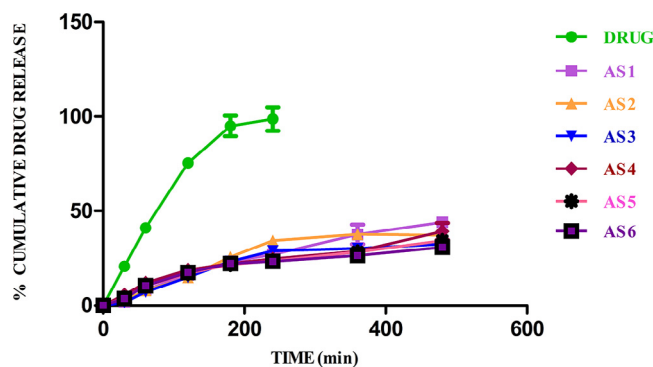


**Fig. 6 – In vitro release profile of acetazolamide from chitosan NPs formulation.**

from chitosan NPs fitted best to Higuchi, which can be confirmed by comparing the values for the regression coefficient ( $R^2$ ) of the zero order, first order, Higuchi, Korsmeyer-Peppas and Hixson Crowell which are 0.83, 0.83, 0.92, 0.91 and 0.82 (calculated from mean values) respectively. The value of 'n' ( $0.5 < n < 1$ ), the diffusion exponent of Korsmeyer-Peppas equation indicated that the release of acetazolamide from CS NPs is anomalous i.e. contributed by combination of dissolution and diffusion.

### 3.1.8. Ex-vivo transcorneal permeation; % corneal hydration

Transcorneal permeation studies through excised goat cornea indicated about 3-fold increase (statistically significant,  $P < 0.05$ ) in permeation of drug from nanosuspension formulation (AS2) compared with an aqueous solution of acetazolamide of same concentration (Fig. 7). The % transcorneal permeation for drug solution was observed  $1.39 \pm 0.01\%$  whereas for different formulations i.e. AS1, AS2, AS3, AS4, AS5 and AS6 it was found to be  $1.18 \pm 0.03$ ,  $2.11 \pm 0.05$ ,  $1.41 \pm 0.03$ ,  $0.76 \pm 0.01$ ,  $0.75 \pm 0.01$  and  $0.73 \pm 0.01$  respectively. The % transcorneal permeation of all the formulations, except, AS3, was found statistically significant ( $P < 0.05$ ) when compared with the transcorneal permeation of plain drug solution. The % corneal hydration was found within the normal range of 75 - 80%, indicating no damage to the cornea during permeation.

### 3.1.9. In-vivo ocular hypotensive efficacy studies

The observation suggested that the hypotensive activity of drug loaded NP formulations (AS2) was comparable to that of the plain drug solution (positive control) (Fig. 8). In case of plain

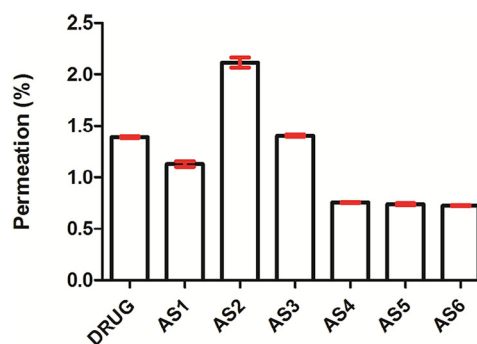


**Fig. 7 – Ex-vivo transcorneal permeation.**

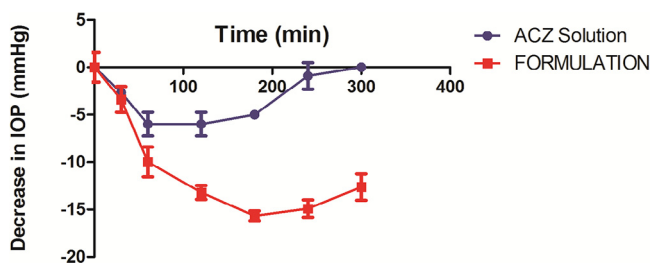


**Fig. 8 – Ocular hypotensive activity of acetazolamide from aqueous solution and optimised chitosan nanoformulation.**

ACZ solution the IOP was decreased for a period of 2 h and then started rising whereas in case of nanoformulations this fluctuation was not observed, the IOP was below the normal level throughout the period of study i.e. 5 h.

### 3.1.10. *In-vitro mucoadhesion studies*

The mucoadhesive strength or bioadhesive force of CS-NPs (AS2) was determined by adsorption of CS-NPs on pig mucin glycoprotein and found to be excellent, i.e.,  $90.34 \pm 1.12\%$  for ACZ loaded CS-NPs.

### 3.1.11. *Stability studies*

The optimized formulation (AS2) made with 1:2 drug-polymer ratio showed around  $97.07 \pm 1.73\%$  acetazolamide content on storage under accelerated condition (i.e.  $40^\circ\text{C}/75\% \text{RH}$ ) for 6 months, while following storage at room temperature for 12 months the drug content was around  $96.45 \pm 3.46\%$ .

## 3.2. Discussion

The nanoparticles were successfully synthesized by interaction of chitosan and STPP. The drug entrapment was calculated by centrifugation of the nanosuspension followed by the measurement of drug content in supernatant. It was observed in formulations that as STPP: CS ratio was amplified, % entrapment of acetazolamide decreased and that is attributed to decreased relative STPP concentration [22]. Zeta potential reveals the electrical potential of particles and is prejudiced by the composition of the particle and the medium in which it is dispersed. The zeta potential of a nanoparticle is dependent on the polyelectrolyte's ratio and is usually used to portray the surface charge of nanoparticles. The particle size of the formulations was found within the range of 161.90–289.40 nm whereas the zeta potential and PDI were found within the range of 24.16–36.86 mV and 0.22–0.32 respectively. All of the nanoparticles are positively charged, but the charge values of AS2 nanoparticles is highest ( $+36.86 \pm 0.70 \text{ mV}$ ) whereas PDI is least ( $0.22 \pm 0.00$ ) which is the indicator of good stability and dispersion homogeneity [31]. Also, as the corneal mucin layer is negatively charged, the positively charged nanoparticles will be mucoadhesive and will increase the ocular bioavailability of the drug. The results of TEM revealed that the prepared nanoparticles were nearly spherical and sub spherical in shape with a smooth surface, devoid of cracks. These particles are not expected to cause any irritation to ocular surface, as it is known that isometric particles with obtuse angles and edges

cause less irritation than particles with sharp angles and edges [28]. Also particles are separated from each other, suggesting that these nanoparticles are possibly stabilized against agglomeration by their strong surface charges. In PXRD studies the presence of sharp peaks in the diffractogram of acetazolamide, mannitol and STPP indicated their crystalline nature while the diffractogram of chitosan indicated amorphous structure. The diffractogram of nanoformulation exhibited the significant peaks which were corresponding to the crystalline structure of mannitol and no peak corresponding to acetazolamide was obtained which indicated the presence of the drug in the amorphous state within the polymer [28]. In FTIR studies the spectrum of nanoformulations didn't show any characteristic peak of ACZ which may be due to excess dilution of ACZ. In DSC studies the thermogram of nanoformulations (AS2) exhibited a small endotherm corresponding to the endotherm of Mannitol and no endotherm of the drug was obtained which may be due to the decreased crystallinity in the formulations or due to the presence of very small quantity of drug in the lyophilized powder [28]. The results of in vitro studies indicated that as the drug: polymer ratio is changed from 1:1 to 1:3 (i.e. as the polymer concentration is increased) the drug release is sustained. The entrapment of the drug in the nanoparticles hinders the drug release. The optimized formulation showed initial burst release for first 2 h of release study (25.64%) followed by sustained release. The initial fast release of acetazolamide can be attributed to rapid hydration of NPs due to the hydrophilic nature of CS as well as drug present at the surface of the particles. Sustained effect can be explained by the presence of the drug within the core of the particles. The release medium penetrates into the particles and dissolves the entrapped drug which further diffuses out into the dissolution media. The results of ex-vivo transcorneal permeation advocate possible corneal uptake of the NPs due to positive charge and small size. Corneal hydration remained in the normal range of 75–80% which showed the eye friendly behaviour of developed formulation [32]. The nanoformulation was found mucoadhesive which is due to hydrogen bond formed between positive charge amino group of chitosan and oligosaccharide chains of mucin [33].

## 4. Conclusion

Acetazolamide, in spite of being one of the most preferred drugs in case of ocular hypertension by the oral route, is the non compliant drug due to its several systemic side effects. Therefore topical alternatives of acetazolamide or topical administration of acetazolamide is required so as to have the compliant dosage form with minimal of side effects. Acetazolamide loaded chitosan nanoparticles can serve the purpose as an alternative to the conventional oral dosage form. The developed optimized formulation exhibited promising results of entrapment, drug release, homogeneity, mucoadhesion, ocular hypotensive activity as well as stability. On the contrary, earlier approaches were unable to get the result to show the significant effect especially when it comes to the use of very low drug concentration in the present study. Hence, treatment of ocular hypertension by this sustained release formulation can be adopted in future.



## Conflicts of interest

The authors declare that there are no conflicts of interest.

## Acknowledgement

Authors are thankful to Prof. D. K. Majumdar (Apeejay Satya University) for his cooperation and Prof. K. Sreenivas, Director, University Science Instrumentation Centre (USIC), University of Delhi (North campus), Delhi (India) for allowing to use TEM and PXRD facilities.

## REFERENCES

- [1] Sahoo SK, Dilnawaz F, Krishnakumar S. Nanotechnology in ocular drug delivery. *Drug Discov Today* 2008;13:144–151.
- [2] Aggarwal D, Pal D, Mitra AK, et al. Study of the extent of ocular absorption of acetazolamide from a developed niosomal formulation, by microdialysis sampling of aqueous humor. *Int J Pharm* 2007;338:21–26.
- [3] Guinedi AS, Mortada ND, Mansour S, et al. Preparation and evaluation of reverse-phase evaporation and multilamellar niosomes as ophthalmic carriers of acetazolamide. *Int J Pharm* 2005;306:71–82.
- [4] Granero GE, Maitre MM, Garnero C, et al. Synthesis, characterization and in vitro release studies of a new acetazolamide-HP- $\beta$ -CD-TEA inclusion complex. *Eur J Med Chem* 2008;43:464–470.
- [5] Kaur IP, Smitha R, Aggarwal D, et al. Acetazolamide: future perspective in topical glaucoma therapeutics. *Int J Pharm* 2002;248:1–14.
- [6] Mishra V, Jain NK. Acetazolamide encapsulated dendritic nano-architectures for effective glaucoma management in rabbits. *Int J Pharm* 2014;461:380–390.
- [7] Medina LS, González-Gómez A, Sousa RO, et al. Chitosan-tripolyphosphate nanoparticles as *Arrabidaea chica* standardized extract carrier: synthesis, characterization, biocompatibility and antiulcerogenic activity. *Int J Nanomedicine* 2015;10:3897–3909.
- [8] Ramin B, Li Y, Jin W, et al. Food hydrocolloids preparation and optimization of pickering emulsion stabilized by chitosan-tripolyphosphate nanoparticles for curcumin encapsulation. *Food Hydrocoll* 2016;52:369–377.
- [9] Mohammadpourounighi N, Behfar A, Ezabadi A, et al. Preparation of chitosan nanoparticles containing *Naja naja oxiana* snake venom. *Nanomedicine* 2010;6:137–143.
- [10] Calvo P, Lopez CR, Vila-Jato JL, et al. Novel hydrophilic chitosan-polyethylene oxide nanoparticles as protein carriers. *J Appl Polym Sci* 1997;63:125–132.
- [11] Yang W, Fu J, Wang T, et al. Chitosan/sodium tripolyphosphate nanoparticles: preparation, characterization and application as drug carrier. *J Biomed Nanotechnol* 2009;5:591–595.
- [12] Berthold A, Cremer K, Kreuter J. Preparation and characterization of chitosan microspheres as drug carrier for prednisolone sodium phosphate as model for antiinflammatory drugs. *J Control Release* 1996;39:17–25.
- [13] Chen R, Qian Y, Li R, et al. Methazolamide calcium phosphate nanoparticles in an ocular delivery system. *Yakugaku Zasshi* 2010;130:419–424.
- [14] Jonassen H, Kjøniksen A, Hiorth M. Stability of chitosan nanoparticles cross-linked with tripolyphosphate. *Biomacromolecules* 2012;13:3747–3756.
- [15] Manchanda S, Sahoo PK, Majumdar DK. RP-HPLC method development and validation for the estimation of acetazolamide in bulk drug and formulations with forced degradation studies. *Der Pharm Lett* 2016;8:338–347.
- [16] Varma VNSRK, Maheshwari PV, Navya M, et al. Calcipotriol delivery into the skin as emulgel for effective permeation. *Saudi Pharm J* 2014;22:591–599.
- [17] Malhotra M, Majumdar DK. In vitro transcorneal permeation of ketorolac tromethamine from buffered and unbuffered aqueous ocular drops. *Indian J Exp Biol* 1997;35:941–947.
- [18] Mohanty B, Mishra SK, Majumdar DK. Effect of formulation factors on in vitro transcorneal permeation of voriconazole from aqueous drops. *J Adv Pharm Technol Res* 2013;4:210–216.
- [19] Rathore MS, Majumdar DK. Effect of formulation factors on in vitro transcorneal permeation of gatifloxacin from aqueous drops. *AAPS PharmSciTech* 2006;7:3–8.
- [20] Manchanda S, Sahoo PK, Majumdar DK. Effect of formulation factors on transcorneal permeation of acetazolamide from aqueous drops: in vitro and in vivo study. *Asian J Pharm* 2016;10:177–182.
- [21] Ameenuzzafar, Ali J, Bhatnagar A, et al. Chitosan nanoparticles amplify the ocular hypotensive effect of catechol in rabbits. *Int J Biol Macromol* 2014;65:479–491.
- [22] Bhatta RS, Chandasana H, Chhonker YS, et al. Mucoadhesive nanoparticles for prolonged ocular delivery of natamycin: in vitro and pharmacokinetics studies. *Int J Pharm* 2012;432:105–112.
- [23] El-Gazayerly ON, Hikal AH. Preparation and evaluation of acetazolamide liposomes as an ocular delivery system. *Int J Pharm* 1997;158:121–127.
- [24] Singla A, Kaur IP, Garg A, et al. Novel approaches for topical delivery of acetazolamide. *Pharm Technol* 2002;24–34.
- [25] Palma SD, Tartara LI, Quinteros D, et al. An efficient ternary complex of acetazolamide with HP- $\beta$ -CD and TEA for topical ocular administration. *J Control Release* 2009;138:24–31.
- [26] Shinde U, Ahmed MH, Singh K. Development of dorzolamide loaded 6-o-carboxymethyl chitosan nanoparticles for open angle glaucoma. *J Drug Deliv* 2013;2013:562727.
- [27] Prego C, Paolicelli P, Diaz B, et al. Chitosan-based nanoparticles for improving immunization against hepatitis B infection. *Vaccine* 2010;28:2607–2614.
- [28] Katara R, Majumdar DK. Colloids and surfaces B: biointerfaces eudragit RL 100-based nanoparticulate system of aceclofenac for ocular delivery. *Colloids Surf B Biointerfaces* 2013;103:455–462.
- [29] Manchanda S, Sahoo PK. Fabrication and characterization of mucoadhesive topical nanoformulations of dorzolamide HCl for ocular hypertension. *J Pharm Invest* 2017;doi:10.1007/s40005-017-0324-x.
- [30] Rosu M, Bratu I. Promising psyllium-based composite containing TiO<sub>2</sub> nanoparticles as aspirin-carrier matrix. *Prog Nat Sci Mater Int* 2014;24:205–209.
- [31] Cegnar M, Kos J, Kristl J. Cystatin incorporated in poly (lactide-co-glycolide) nanoparticles: development and fundamental studies on preservation of its activity. *Eur J Pharm Sci* 2004;22:357–364.
- [32] Pawar PK, Majumdar DK. Effect of formulation factors on in vitro permeation of moxifloxacin from aqueous drops through excised goat, sheep, and buffalo corneas. *AAPS PharmSciTech* 2006;7:1–6.
- [33] Manchanda S, Sahoo PK, Majumdar DK. Mucoadhesive chitosan-dextran sulphate nanoparticles of acetazolamide for ocular hypertension. *Nanotechnol Rev* 2016;5:445–453.